EDGE TECHNIQUE LIDAR FOR HIGH ACCURACY, HIGH SPATIAL RESOLUTION WIND MEASUREMENT IN THE PLANETARY BOUNDARY LAYER

FINAL REPORT

C. LAURENCE KORB AND BRUCE M. GENTRY

JULY 1, 1995

U. S. ARMY RESEARCH OFFICE

GRANT ARO116-94

NASA
GODDARD SPACE FLIGHT CENTER
LABORATORY FOR ATMOSPHERES, CODE 912
GREENBELT, MD 20771

APPROVED FOR PUBLIC RELEASE ;
DISTRIBUTION UNLIMITED

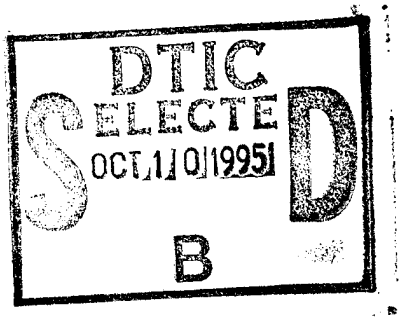

DISCLAIMER NOTICE

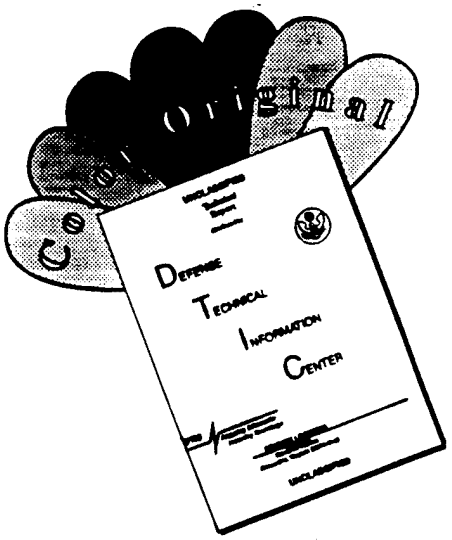

THIS DOCUMENT IS BEST QUALITY AVAILABLE. THE COPY FURNISHED TO DTIC CONTAINED A SIGNIFICANT NUMBER OF COLOR PAGES WHICH DO NOT REPRODUCE LEGIBLY ON BLACK AND WHITE MICROFICHE.

Table of Contents

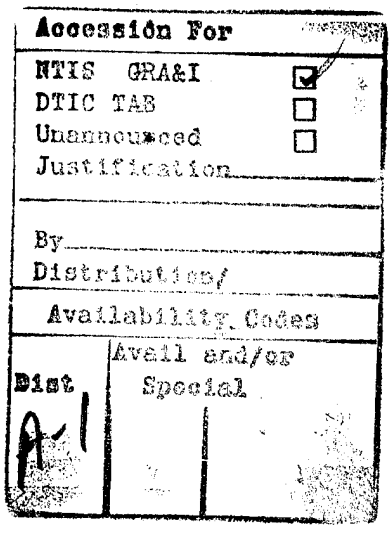

List of Figures

I. Statement of the Problem Studied

The goal of the Army Research Office Geosciences program is to measure the three dimensional wind field in the planetary boundary layer (PBL) over a measurement volume with a 50 meter spatial resolution and with measurement accuracies of the order of 20 cm/sec. The objective of this work is to develop and evaluate a high vertical resolution lidar experiment using the edge technique for high accuracy measurement of the atmospheric wind field to meet the ARO requirements. This experiment allows the powerful capabilities of the edge technique to be quantitatively evaluated. In the edge technique, a laser is located on the steep slope of a high resolution spectral filter. This produces large changes in measured signal for small Doppler shifts. A differential frequency technique renders the Doppler shift measurement insensitive to both laser and filter frequency jitter and drift. The measurement is also relatively insensitive to the laser spectral width for widths less than the width of the edge filter. Thus, the goal is to develop a system which will yield a substantial improvement in the state of the art of wind profile measurement in terms of both vertical resolution and accuracy and will provide a unique capability for atmospheric wind studies.

The wind field is the single most important atmospheric state variable required for understanding atmospheric motion and predicting weather. High spatial and temporal resolution wind measurements from ground-based or airborne remote sensing systems are important in describing the evolution of mesoscale circulations associated with various atmospheric phenomena including deep and shallow convection, density currents and gravity wave activity. The data is extremely important in efforts to understand and model these phenomena. The accuracy and high vertical resolution of the edge technique will also provide a unique capability to directly observe vertical winds at the 10 to 20 cm/sec level which will allow studies of turbulent motion and the evolution of convective cells in the boundary layer. Such measurements could also be applied for detection of wind shear, microbursts, and turbulence -- all of which represent significant aircraft safety hazards.

II. Summary of Results

A. Lidar Development

A ground-based Doppler lidar system was developed under this program to demonstrate the capability of the edge technique to measure atmospheric winds. In the first part of the program, the hardware and software for acquisition of the wind lidar data was developed. This work utilizes our prior work developing the theory and methodology of the edge technique. A brief overview of the methodology of the measurement and a description of the experiment is provided below.

An optical schematic of the lidar system is shown in Figure 1. An injection seeded pulsed Nd:YAG laser is used as the narrowband energy source. The laser has an output energy of up to 800 mJ per pulse at a repetition rate of 10 Hz. The laser pulse length is 15 nsec and we have measured the spectral width of this laser as 35-40 MHz at 1.06 μm which is near transform limited for a Gaussian pulse. The spectral bandwidth of this laser is sufficiently narrow to make the proposed wind measurements with the edge technique.

A small fraction of the outgoing laser signal is picked off and used to make a reference measurement of the laser frequency on the Fabry Perot etalon for each outgoing laser pulse. The beam is first collimated and the divergence is matched to that of the atmospheric backscattered signal collected by the telescope. It is also attenuated to provide signals at the detectors of the same magnitude as those backscattered from the atmosphere. The reference beam is then input to the edge detection setup.

The major portion of the laser energy (99%) is transmitted to the atmosphere via beam steering optics. A portion of the laser energy is backscattered from each range element of the atmosphere and the resultant signal is collected by a reflective telescope with a diameter of 0.4 meters. The

field of view of the telescope is set by a field stop which is adjusted to make the field of view of the telescope greater than or equal to the divergence of the outgoing laser beam. The resultant beam is collimated and transferred to a beamsplitter which combines the atmospheric backscattered and the picked off reference laser signals. The signals are then bandpassed by a narrowband interference filter to reject unwanted background and are then collimated to satisfy the collimation and throughput requirements of the Fabry Perot etalon which is used as the edge filter. The collimated beam is then split between the edge filter and energy monitor paths. Condensing optics focus the beams to minimize the size of the high quantum efficiency solid state avalanche photodiode detectors.

The central fringe of a Fabry-Perot etalon is used as a high resolution edge filter to measure the shift of the aerosol return which has the original sharp spectral distribution of the laser. Various other filters with sharp spectral edges could be used. These include gratings, prisms, and molecular or atomic gas absorption lines. Fabry Perot etalons, plane or spherical, offer much higher resolution (sharper edges) than the other filters and they also have high throughput. In addition the etalon bandpass can be tuned to match the laser frequency which allows existing lasers such as Nd:YAG to be used. Also, a filter with a sharp transmission feature such as an etalon has the advantage of rejecting broadband background sources such as the Rayleigh backscatter or solar background while an atomic or molecular absorption feature would transmit these unwanted background sources.

The edge and energy monitor detector signals are simultaneously sampled as a function of time to provide range resolved information. Two synchronized 12-bit analog to digital converters with sampling rates as high as 20 MHz are used to obtain range resolution as high as 7.5 meters (round-trip). The collected signals are digitized, stored and processed for the Doppler/velocity information.

The laser signal is transmitted coaxially with the telescope by a small flat to beam steering optics located outside our laboratory. The beam steering optics provide the capability to direct the beam

to the atmosphere and to vary the azimuth and elevation angles of the beam. The azimuth and elevation angles are manually adjusted. The beam can be directed from 30 to 120 degrees in elevation angle and from -60 to 60 degrees in azimuth. This allows us to make atmospheric slant path measurements to measure the horizontal components of the wind field as well as to independently measure the vertical component of the wind.

B. Wind measurements

Over the past two years we have built a ground-based lidar system as described. Recently we were successful in integrating and testing the Fabry Perot etalon edge filter in the lidar system. Tests were performed using both a narrowband pulsed and a CW Nd:YAG laser and the results showed the desired high resolution etalon fringes. The etalon had a plate separation of 5 cm yielding a free spectral range of 0.1 cm^{-1} and a plate reflectivity of 93.5 % giving a theoretical finesse of 47 and a theoretical resolution (FWHH) of 65 MHz. The observed fringes for the CW laser (linewidth < 100 kHz) had a measured finesse as high as 44. The fringes observed for the atmospheric backscattered aerosol signal had a finesse of 30 which is in good agreement with theory when the pulsed laser linewidth of 40 MHz and the effects of finite angular field of view are included. A finesse of 30 corresponds to a total instrument resolution (FWHH) of 100 MHz giving a sensitivity of 4% per m/s at the half-width of the fringe.

In order to make wind measurements on the edge, a servo control system was developed to lock the edge of the etalon fringe to the pulsed Nd:YAG laser frequency. The reference measurement of the outgoing laser frequency on the edge is compared to a setpoint value, for instance the half-width. A deviation from the setpoint value generates a small error signal which is applied to tune the etalon to compensate for the deviation. The purpose of this system is to keep the laser frequency at approximately the correct location on the edge. Very high frequency stability is not required since a differential frequency measurement is made. That is, the frequency of the atmospheric backscattered signal from each range gate is measured relative to the frequency of the outgoing laser signal, the reference measurement, for each pulse. The time history of

measurements on the edge at a fixed altitude of 800 m is shown in Figure 2 for a 10 shot average and a range resolution of 22.5 m. The normalized signals (I_{EDG}/I_{EM}) for the atmosphere and the corresponding signals for the outgoing reference frequency are shown along with the difference signal. As may be seen, the reference measurement on the edge varies as a function of time. However, the atmospheric measurements track the reference measurements and by taking the difference between these the pulse-to-pulse frequency variations due to the laser or the filter are removed. The difference measurement is proportional to the Doppler shift and contains the wind information.

Figure 3 shows our first wind profile measurements which were made on April 26, 1994. The data are for a 100 shot average and a range resolution of 22.5 m which yields a vertical resolution of approximately 15 meters. The measurements are for the radial component of the wind along the line of sight of the laser in the east-west direction. The Nd:YAG laser has an output energy of up to 800 mJ per pulse. The laser energy actually used for the wind measurements was limited to 120 mJ to avoid damaging the metallic coatings on the 40 cm diameter atmospheric beam steering mirror. The measurements were made by manually steering the atmospheric output mirror to direct the beam at an elevation angle of 45 degrees first toward the east and then towards the west. The east-west component of the wind was found by taking half of the difference in the measured line of sight winds for the two directions. The rms error of the data is approximately 0.25 m/s which corresponds to a peak-to-peak variation of 1.25 m/s.

In the last six months of the second year of this program, we made measurements with the Edge Technique Lidar system which demonstrate some of the unique capabilities of our system. Three different types of measurements were obtained:

1) hard target measurements which provide zero velocity validation of the lidar;
2) profiles of vector winds i.e. horizontal wind speed and direction and comparison of the lidar wind profiles with rawinsonde measurements from Dulles airport.
3) line-of-sight wind profiles as a function of time which provide a high resolution view of the temporal evolution of winds and turbulence in the boundary layer.

The hard target measurements were undertaken in order to provide a zero velocity calibration measurement which is a pivotal point for the lidar instrument. This meaurement allows us to determine if there are any systematic instrument effects and provides a statistical measurement of the lidar accuracy for zero velocity.

The normalized edge signals measured by the lidar system are shown in Figure 4 as a function of time. Each measurement represents a 100 shot average (10 seconds). The data represented by circles are the reference measurements of the outgoing laser frequency. These are made by locating the position of the outgoing laser frequency on the edge of the spectral response function of the Fabry-Perot etalon edge filter. The triangles correspond to zero velocity hard target measurements obtained from trees located about 50 meters from the lidar. The position of the laser on the edge is held constant from shot to shot by locking the etalon to the laser frequency with a servo control loop. This eliminates sensitivity to frequency instabilities of the laser or the etalon. We have demonstrated locking the etalon to the laser in the presence of large frequency drifts (equivalent to > 100 m/s velocity) for many hours of continuous operation. This is described in our recent *Applied Optics* paper. As shown in Figure 4, the lidar hard target return overlays the reference data very closely and tracks its value as the reference varies slightly from measuremnt to measurement. This is what one would expect to see for a zero velocity target (i.e. no Doppler shift).

Figure 5 shows the velocity measurements resulting from the hard target measurements. The Doppler shift, and thus the wind, is determined by taking a difference between the target and reference measurements (see Figure 4) and dividing by the sensitivity (slope) of the edge at the position of the measurement. The sensitivity for this experiment is 3% per m/sec. That is, a 1 m/sec wind produces a change in measured signal of 3% . The absolute accuracy of these measurements is very high with a mean offset of only 19 cm/s and a rms standard deviation of only 17 cm/s. The excellent agreement of these data with the zero velocity hard target indicate that the lidar system is performing as expected and that systematic effects are small.

Figure 6 is an example of a wind profile obtained with the lidar system showing wind speed and direction as a function of altitude. The horizontal wind speed and direction are obtained by analyzing two line-of-sight wind profile measurements taken at 45° elevation angle with a 90° difference in azimuth angle i.e. one profile is taken pointing to the East with a second profile pointing to the North. The data are for a 100 shot average (10 seconds) and a vertical resolution of 26 meters (37.5 m range resolution). We estimate from the signal-to-noise in the data that the accuracy of these wind measurements is about 20 cm/s. The Dulles airport rawinsonde wind profiles taken at 1200 Z and 0000 Z on the same day are also shown in the figure for comparison. The rawinsonde profiles show only modest variations during the 12 hour interval between measurements which indicates fairly stable synoptic scale conditions prevailed. Under these conditions the Dulles measurements probably are representative of the winds at Goddard. Very good agreement is observed between the lidar and rawinsonde measured winds.

Figure 7 shows a three dimensional view of the wind as a function of range (altitude) and time obtained by pointing the lidar in one direction (North) at a 45° elevation angle and accumulating profiles every 10 seconds. These data represent a 100 shot (10 second) average and a vertical resolution of 26 meters. The surface thus gives a picture of the time history of the line-of-sight wind and turbulence in the atmosphere with extremely high spatial and temporal resolution. Each individual wind profile shows a variation of the wind with range (altitude) with several prominent wind shear features clearly evolving during the observation time of about 5 minutes. The rapidly evolving dynamic nature of the planetary boundary layer is well described. The figure clearly shows the evolution of the wind field in the temporal and spatial domains.

The last group of figures, Figures 8-16, shows the line-of sight wind data in more detail by displaying the individual profiles in groups of 3 consecutive measurements, one taken every 10 seconds. The starting time of the measurements is shown in the upper right hand corner. The circles are wind profile data which result from the first 10 second average, the stars are the next 10 second average (20 seconds elapsed time) and the triangles are the third 10 second average (30 seconds elapsed time). The vertical resolution is still 26 meters. This more conventional 2-dimensional display of the

data gives a clear picture of the rapidly varying structure of the wind field. The evolution of distinct shear layers is readily apparent. These features are observed from one independent profile to the next. Of particular interest is the evolution of the wind shear feature near 850 m for times from 4:49 to 4:52. The various shear features show slow and consistent variation which is both scientifically interesting and indicates the validity of the data since this type of slowly varying structure along independent profiles is not consistent with any systematic instrumental effects. Figure 7 also clearly shows the evolution of the wind shear feature near 850 m.

III. List of Publications

Refereed

C. Laurence Korb, B. Gentry , and C. Y. Weng, "The Edge Technique - Theory and Application to the Lidar Measurement of Atmospheric Winds", *Appl. Opt.*, **31**, 4202-4212, 1992.

Bruce Gentry and C. L. Korb, "Edge Technique for high accuracy Doppler velocimetry", *Appl. Opt.*, **33**, 5770-5777, 1994.

Invited

C. Laurence Korb, G. K. Schwemmer and B. Gentry, "Lidar Remote Sensing of Pressure, Temperature and Wind" , Invited Paper, 1993 Annual Meeting of the Optical Society of America / 9 th International Laser Society, Toronto, Canada, October, 1993.

Other

C. Laurence. Korb and B. Gentry,"Ground and spaceborne lidar wind measurement with the edge technique", Proceedings of the Coherent Laser Radar Conference, Paris, July, 1993, pp 266-269.

Bruce Gentry, C. L. Korb, and S. X. Li, "Ground-based Lidar Wind Measurement With the Edge Technique", Proceeding of the 17th International Laser Radar Conference, Sendi, Japan, July, 1994.

C. Laurence Korb, B. Gentry, and S. X. Li, "High Spatial Resolution Atmospheric Wind Measurements with the Edge Technique", Proccedings of the OSA Topical Meeting on Optical Remote Sensing of the Atmosphere, Salt Lake City, UT, Feb. 1995.

IV. Report of Inventions

C. Laurence Korb, "Edge Technique for measurement of laser frequency shifts including the Doppler shift", U.S. Patent No. 5,216,477 awarded June, 1993.

V. Bibliography

Abreu, V., Appl. Opt., **18**, 2992-2997 (1979).

Bayer-Helms, F., Z. Angew. Physik, **15**, 330-338 (1963).

Bilbro, J., G. Fichtl, D. Fitzjarrald, M. Krause and R. Lee, Bull. Am. Meteor. Soc., **65**, 348-359 (1984).

Born, M. and E. Wolf, *Principles of Optics*, 6th edition, Pergamon Press (1980).

Gentry, B. and C. L. Korb, "Edge Technique for High Accuracy Doppler Velocimetry", Appl. Opt., **33**, 5770-5777.

Grund, C. and E. Eloranta, Appl. Opt., **30**, 2668-2670, 1991.

Hays, P. , V. Abreu, J. Sroga, and A. Rosenberg, *Conference on Satellite Remote Sensing and Applications*, AMS, Clearwater, FL, June, 1984.

Hernandez, G., Appl. Opt., **5**, 1745-1748 (1967).

Jacquinot, P., J. Opt. Soc. Am., **44**, 761-765 (1954).

Kane, T., W. Kozlovsky, R. Byer and C. Byvik, Opt. Lett., **12**, 239-241 (1987).

Kane, T., B. Zhou, and R. Byer, Appl. Opt., **23**, 2477-2481 (1984).

Kavaya, M., S. Henderson, J. Magee, C. Hale, and R. M. Huffaker, Opt. Lett., **14**, 776-778 (1989).

Kingston, R. H. , *Detection of Optical and Infrared Radiation*, Springer-Verlag (1978).

Korb, C.L. and B. Gentry, invited paper given at *Conference on Lasers and Electro-Optics*, Los Angeles, CA, May, 1990.

Korb, C.L. , B. Gentry and C.Y. Weng ,"The Edge Technique- Theory and Application to the Lidar Measurement of Atmospheric Wind", Appl. Opt., 31, 4202-4213, 1992.

McClatchey, R. A. , R. Fenn, J. Selby, F. Volz, J. Garing, *Optical Properties of the Atmosphere, 3rd Ed* , ARCRL Environmental Research Paper AFCRL 72-0479 (1972).

Post, M. J. and R. E. Cupp, Appl. Opt. , **29**, 4145-4158, 1990.

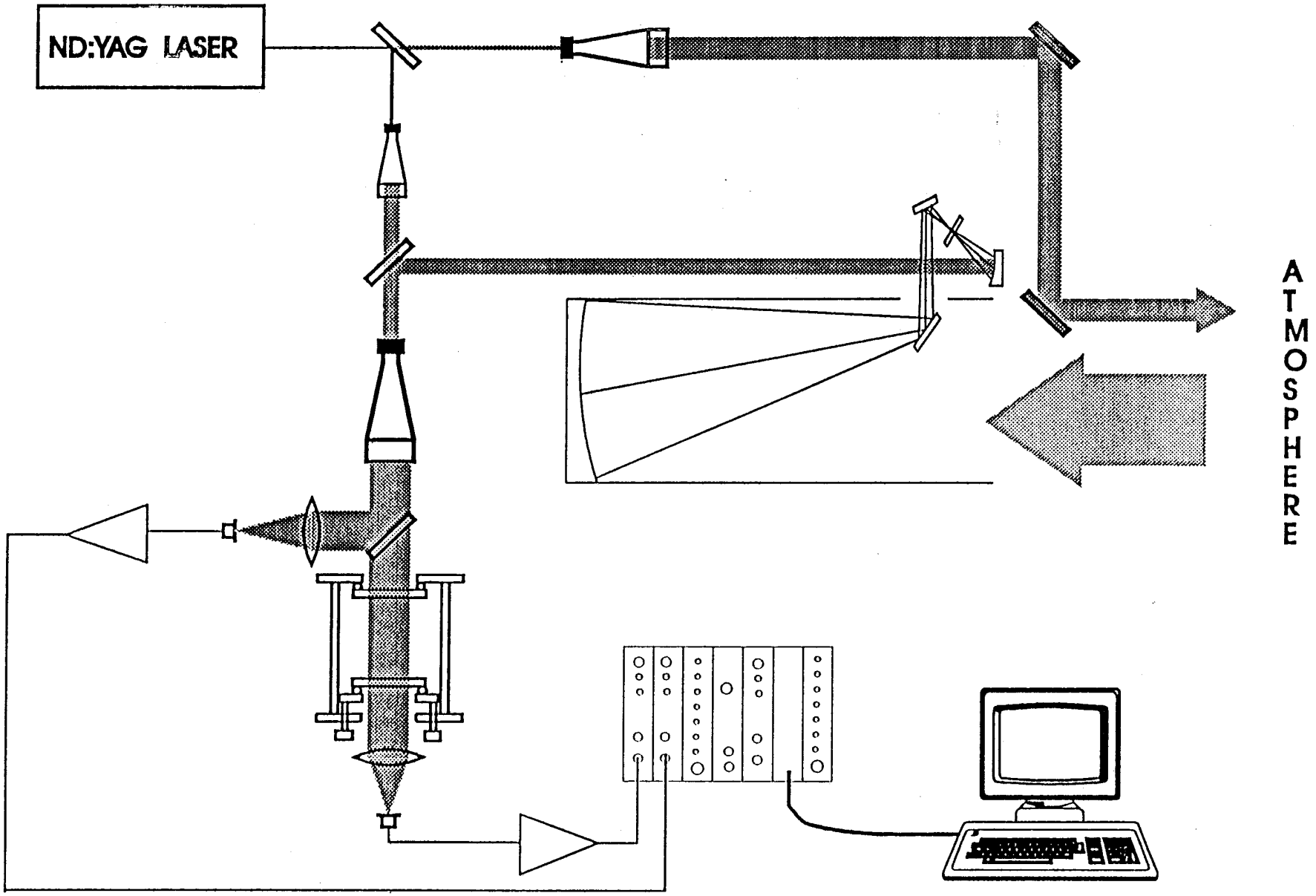

Figure 1 - Optical schematic of the edge technique lidar system.

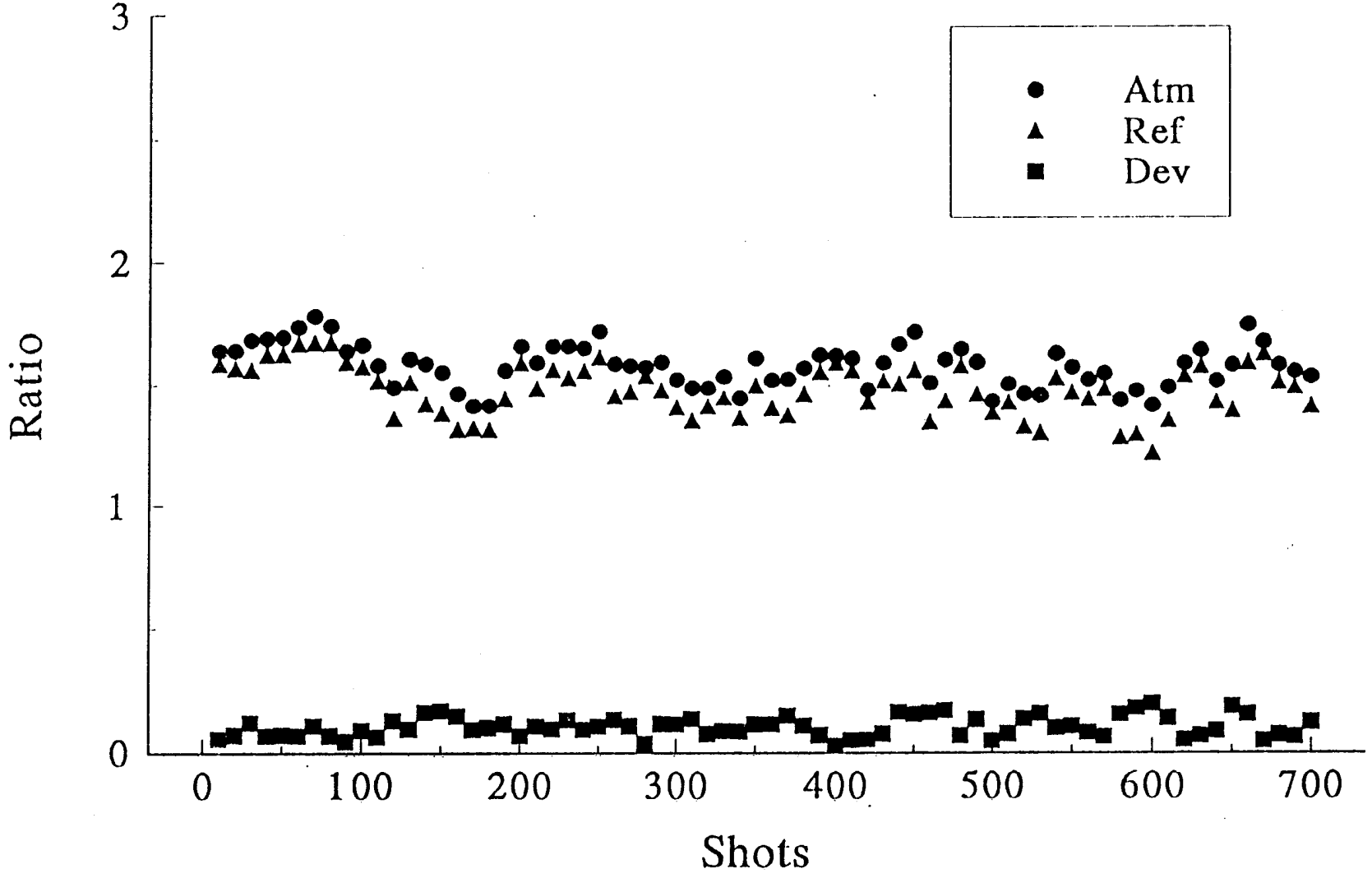

Figure 2 - Normalized edge signals for the outgoing laser frequency reference measurement and for the atmospheric return from an altitude of 800 m. Each data point is determined from a 10 shot average. The difference (Dev) contains the Doppler shift information from which the wind is determined.

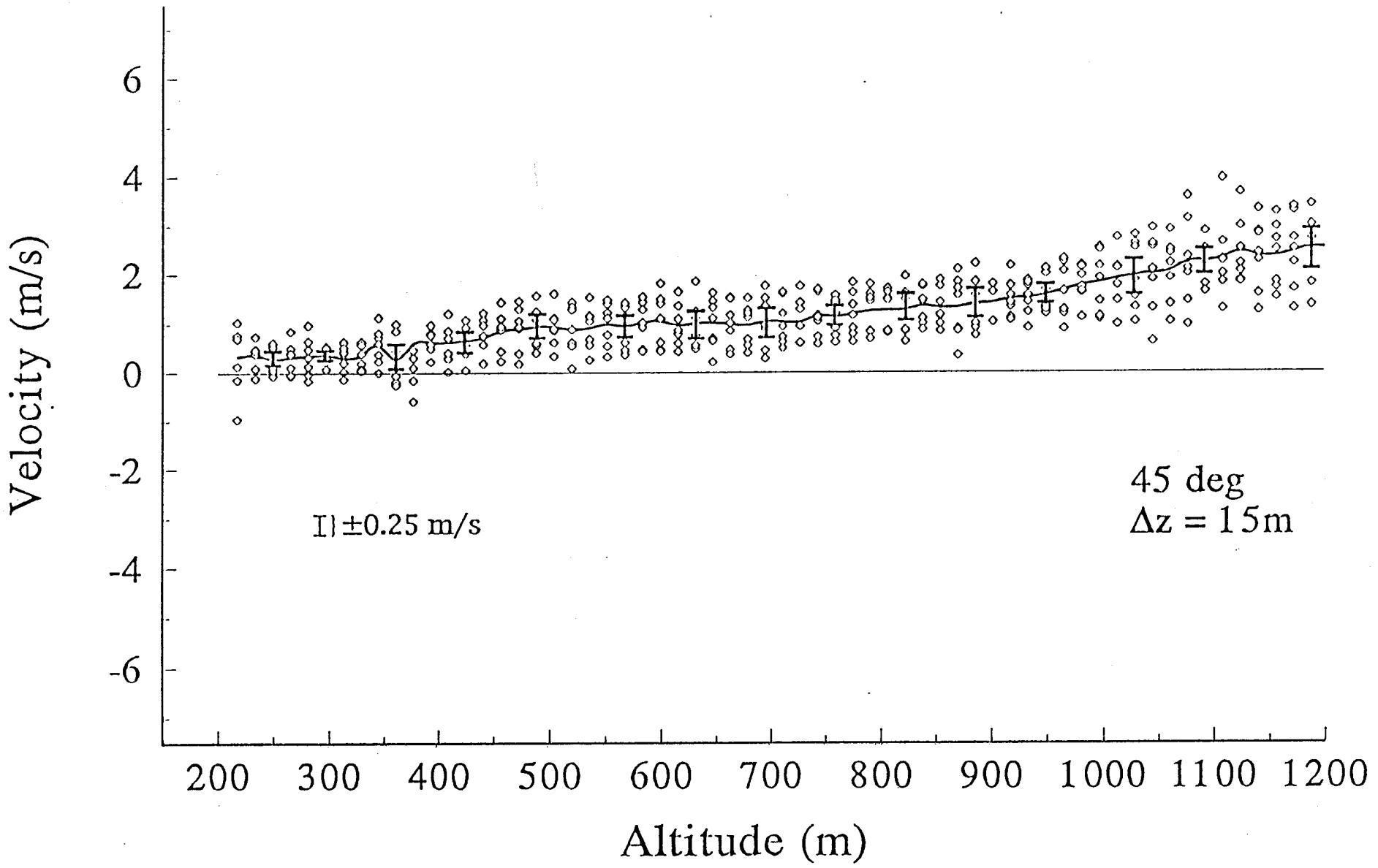

Figure 3 - East-West radial wind profile measurements obtained with the edge technique lidar. The data are for a vertical resolution of 15 m, a 100 shot average, a 45 deg elevation angle and a laser energy of 120 mJ.

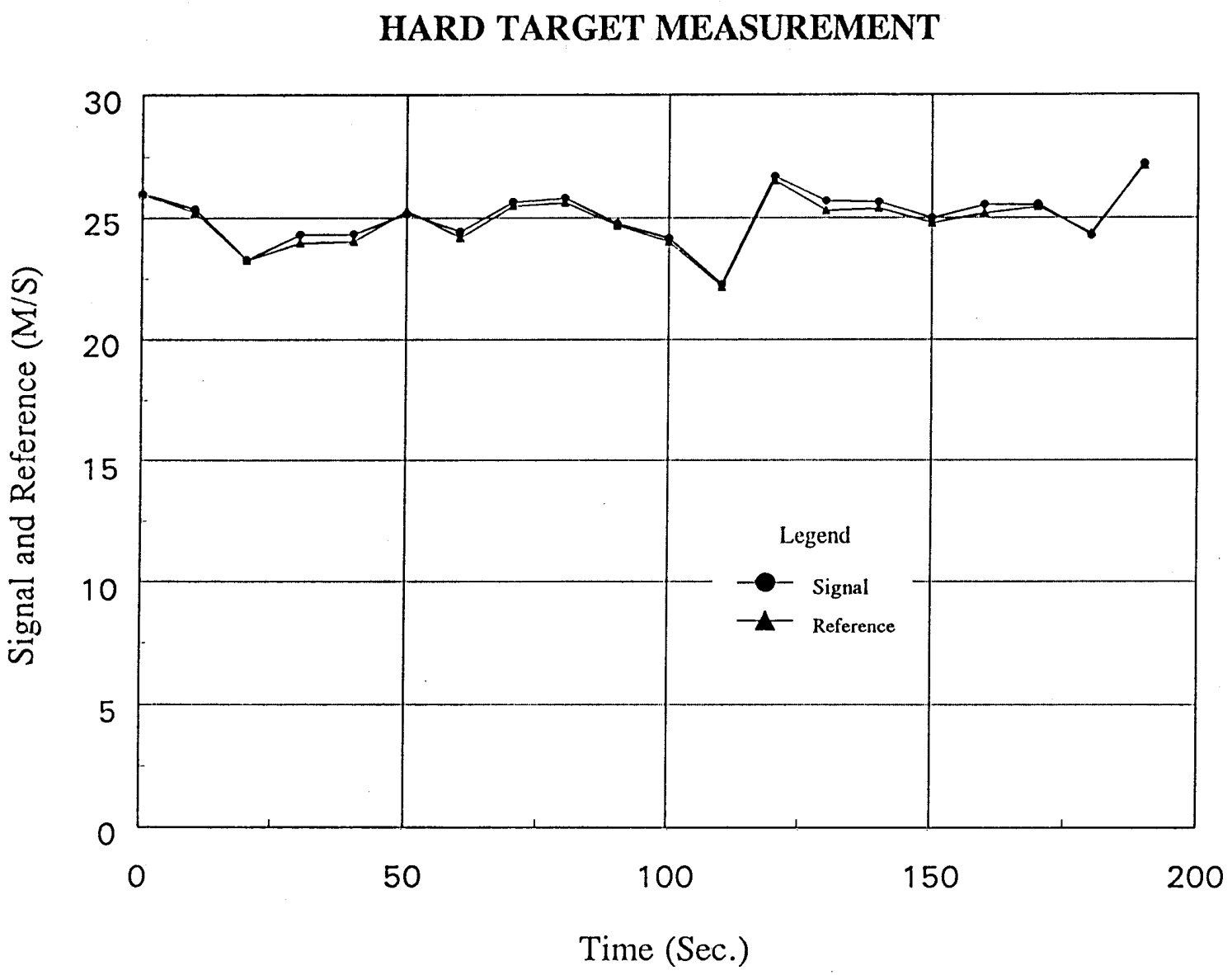

Figure 4 - Edge signals for the outgoing reference and a stationary hard target are shown as a function of time. Each measurement is a 100 shot average.

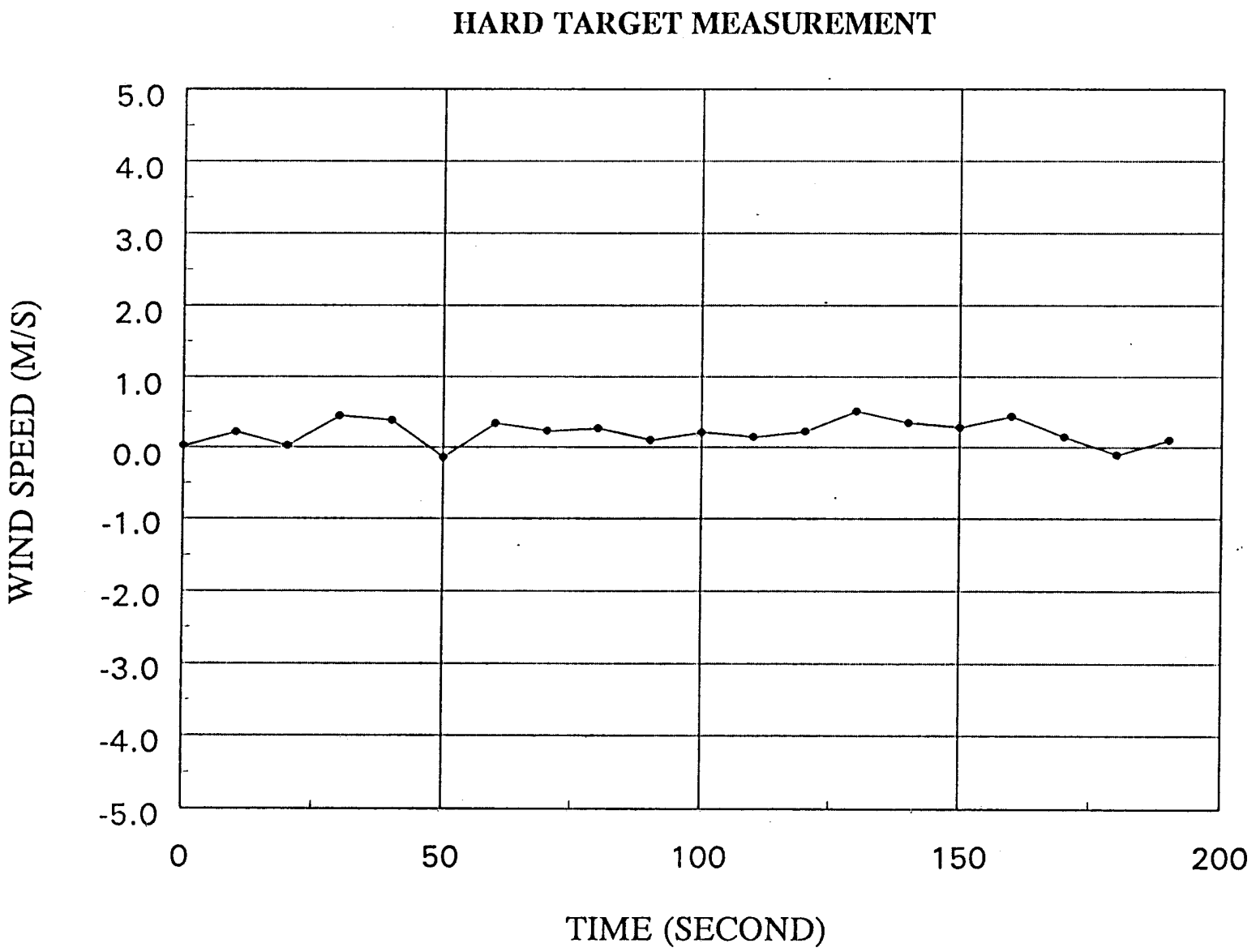

Figure 5 - Velocity measurement determined for a stationary hard target.

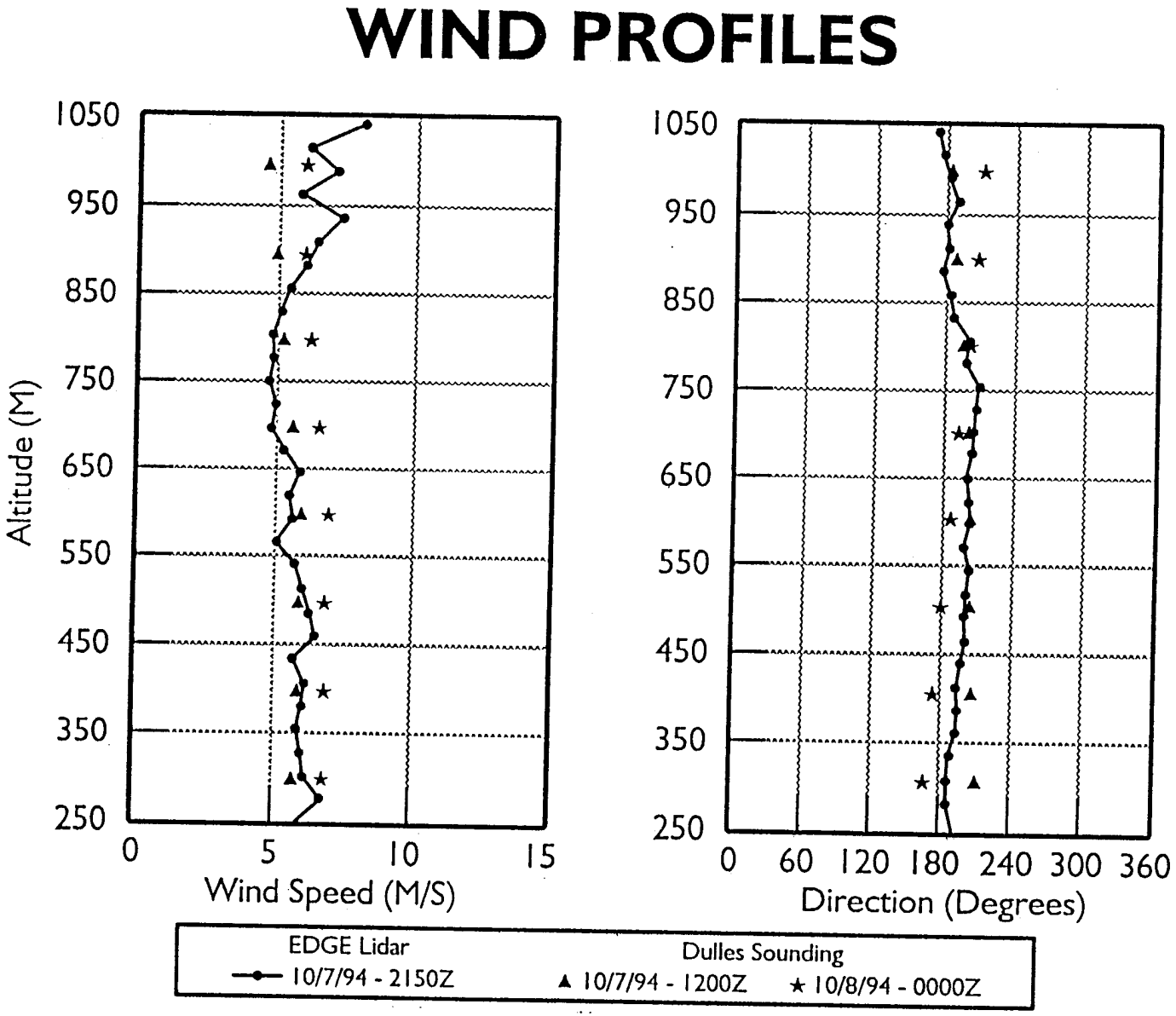

Figure 6 - Lidar profiles of wind speed and direction obtained with the edge technique lidar. Rawinsonde profiles taken at Dulles airport on the same day are shown for comparison.

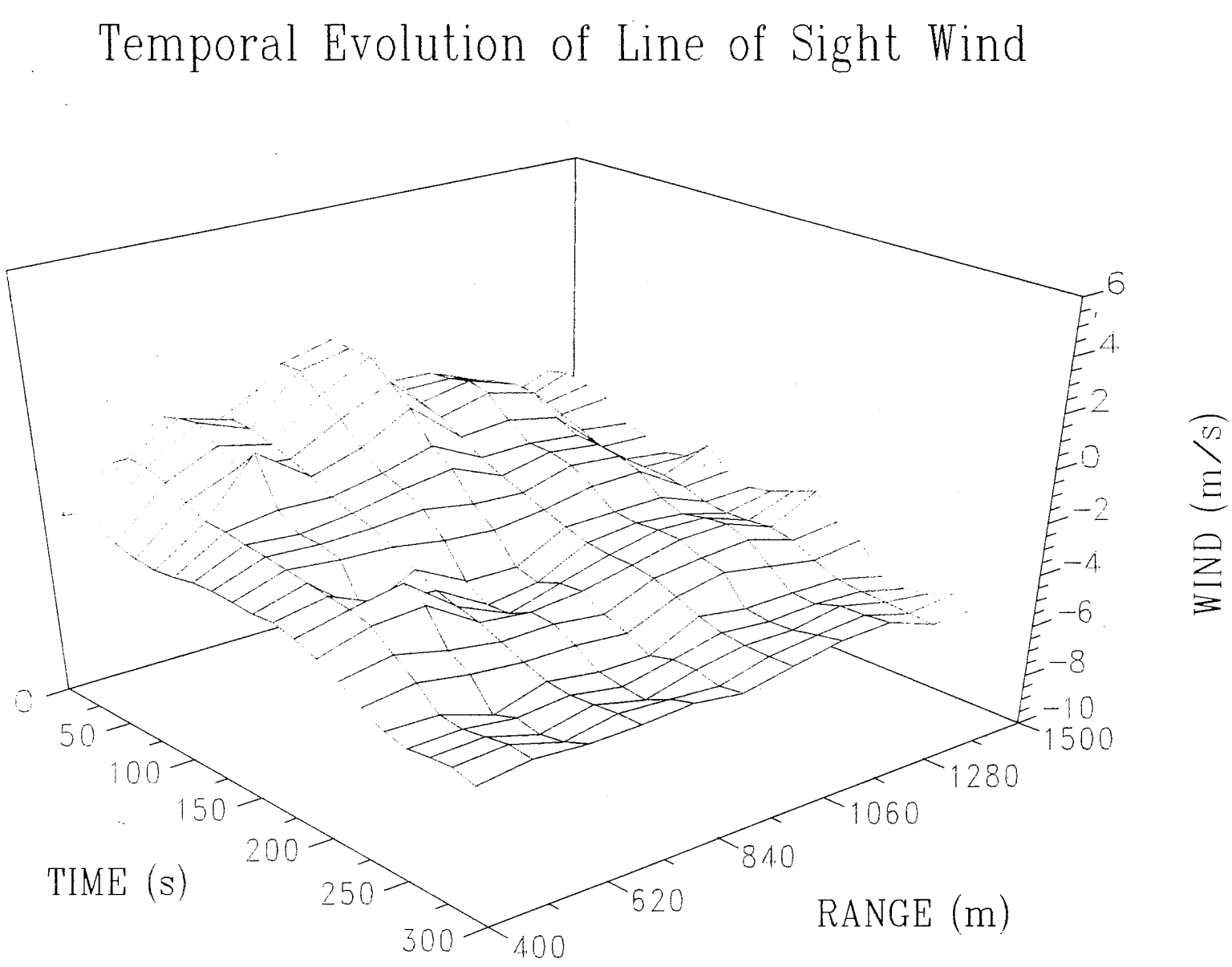

Figure 7 - Line of sight winds taken with edge lidar showing temporal evolution of winds and turbulence in the planetary boundary layer. The vertical resolution is 26 meters and each profile is determined from a 10-second average.

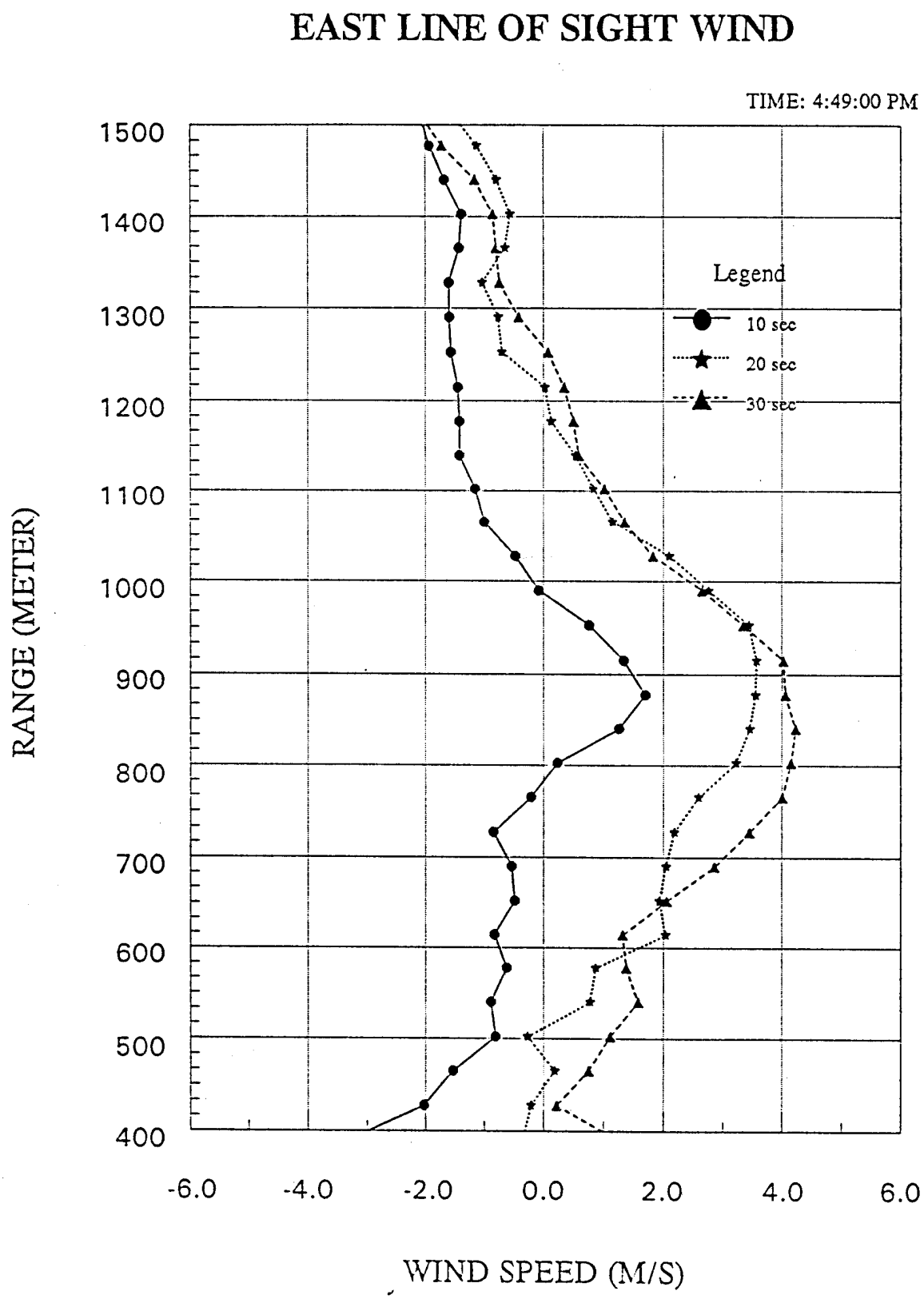

Figure 8 - Line of sight wind profiles obtained with the edge technique lidar. Three consecutive profiles, each taken from a 10-second average, are shown beginning at 4:49:00 p.m.

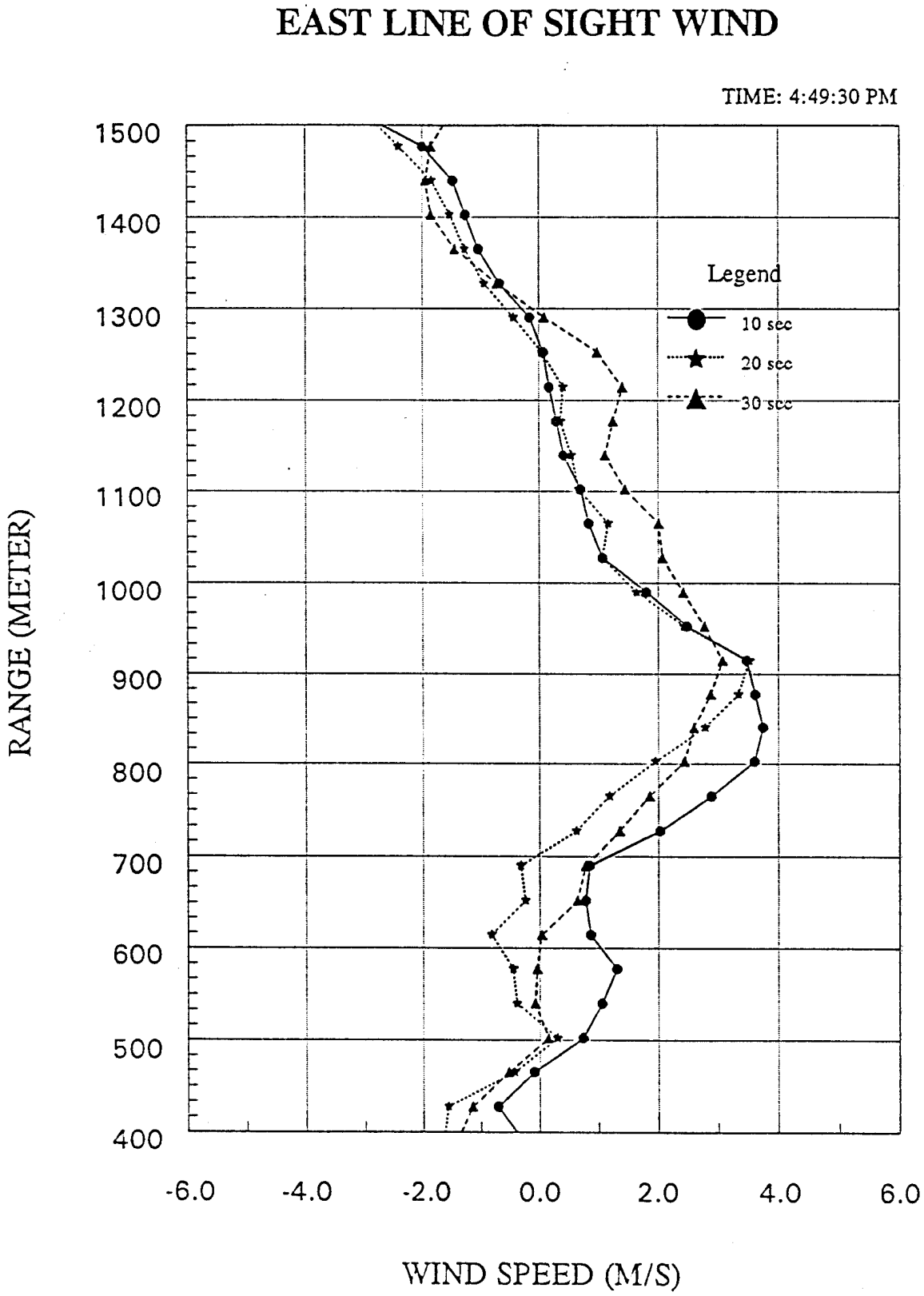

Figure 9 - Line of sight wind profiles obtained with the edge technique lidar. Three consecutive profiles, each taken from a 10-second average, are shown beginning at 4:49:30 p.m.

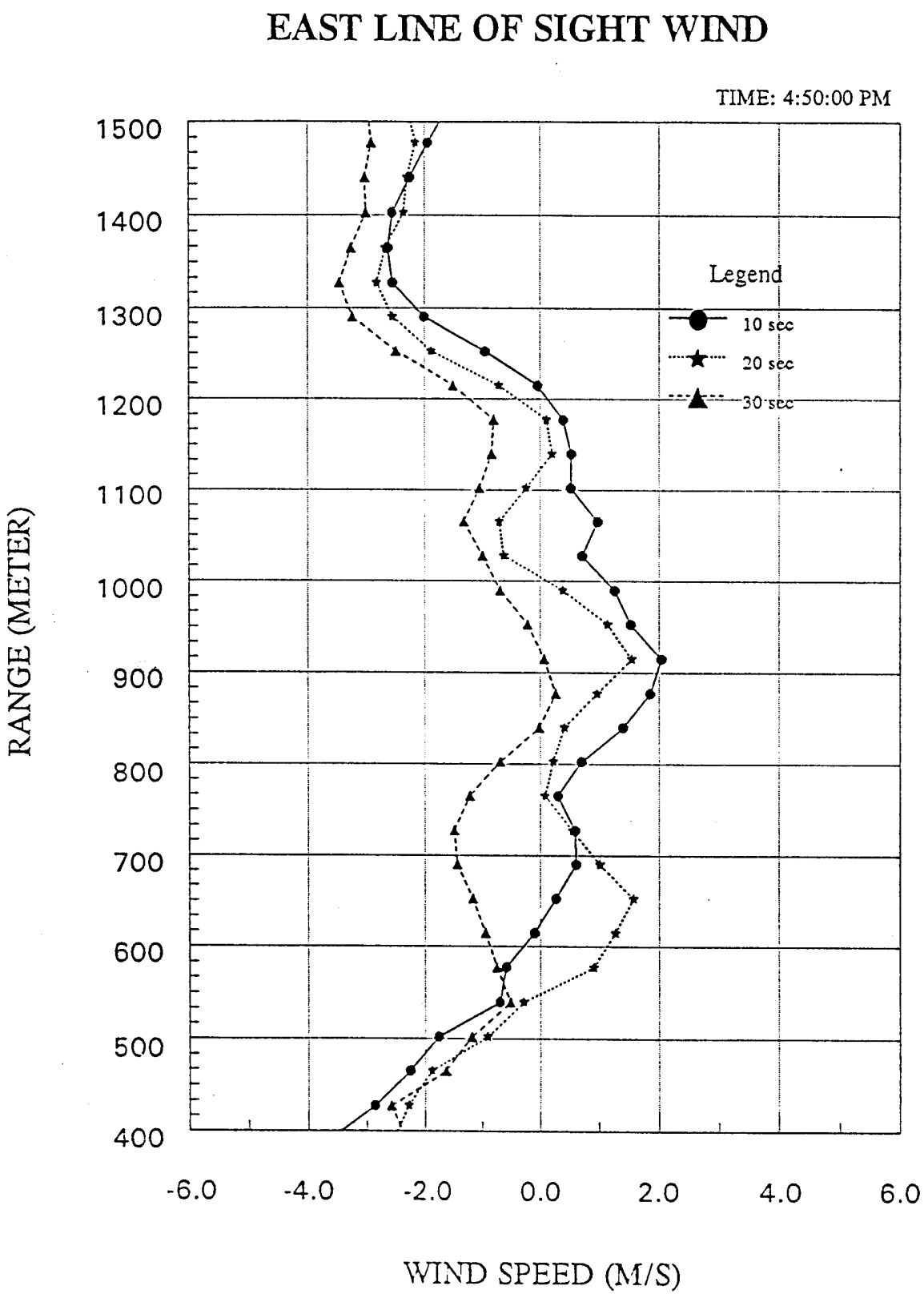

Figure 10 - Line of sight wind profiles obtained with the edge technique lidar. Three consecutive profiles, each taken from a 10-second average, are shown beginning at 4:50:00 p.m.

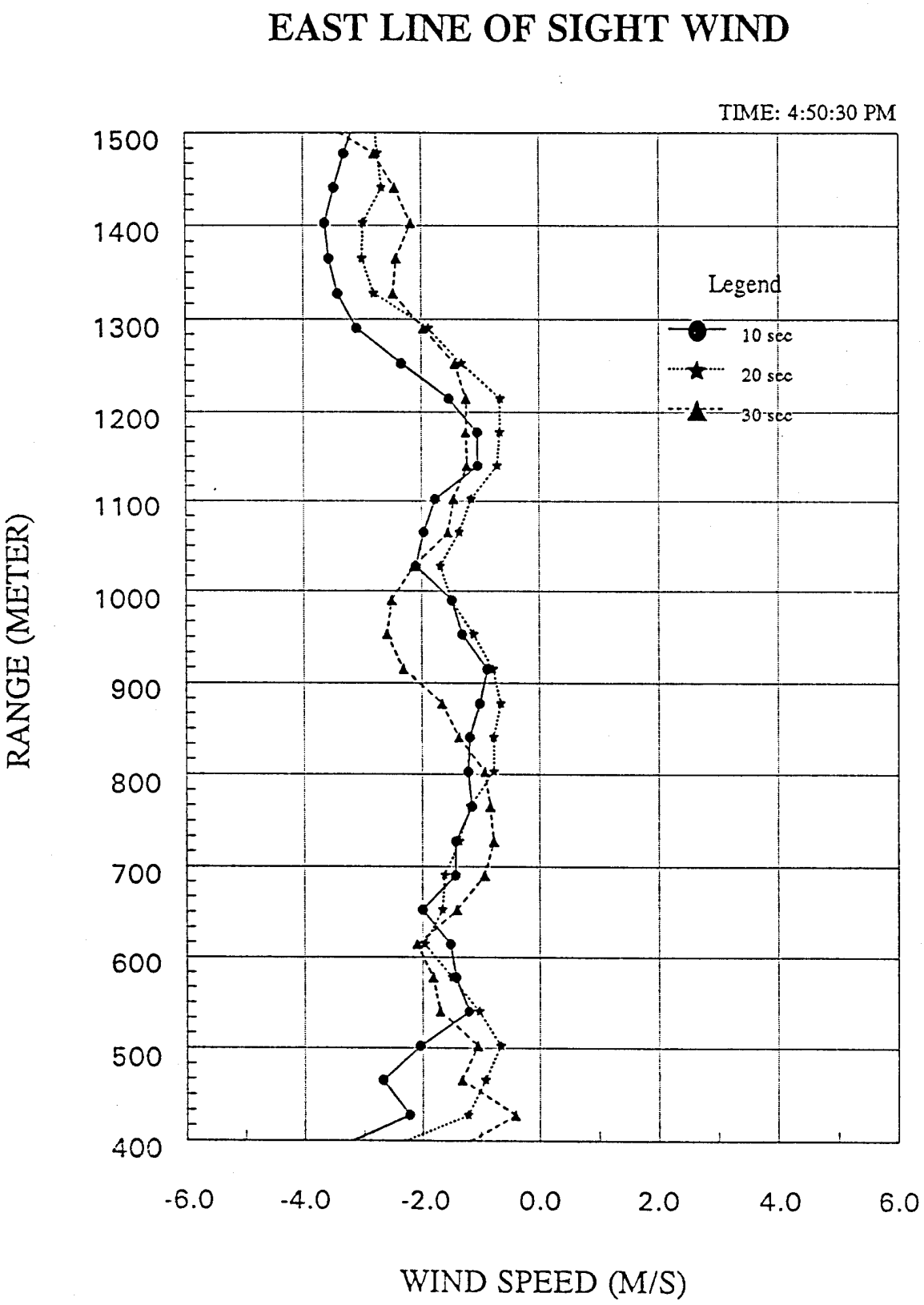

Figure 11 - Line of sight wind profiles obtained with the edge technique lidar. Three consecutive profiles, each taken from a 10-second average, are shown beginning at 4:50:30 p.m.

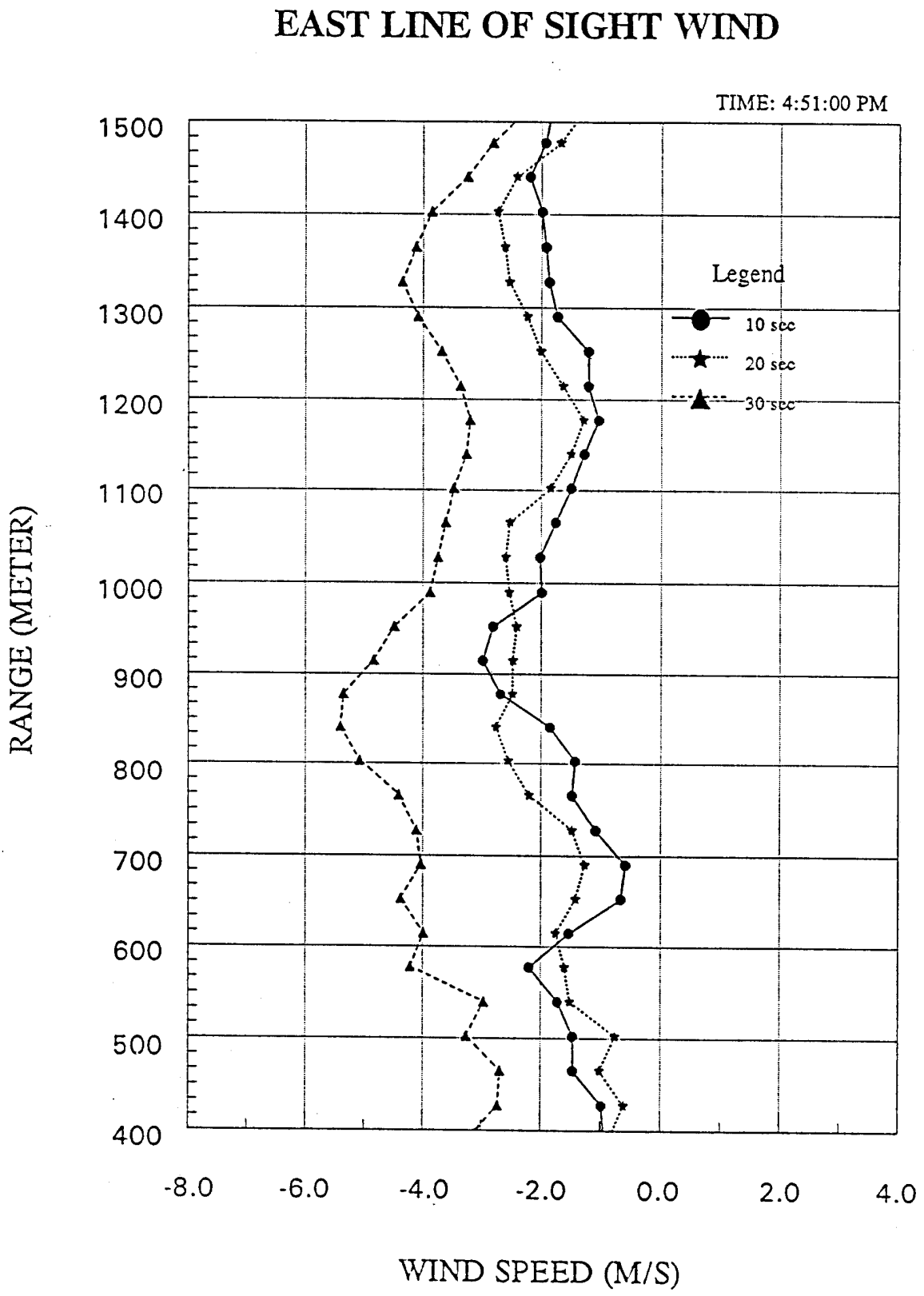

Figure 12 - Line of sight wind profiles obtained with the edge technique lidar. Three consecutive profiles, each taken from a 10-second average, are shown beginning at 4:51:00 p.m.

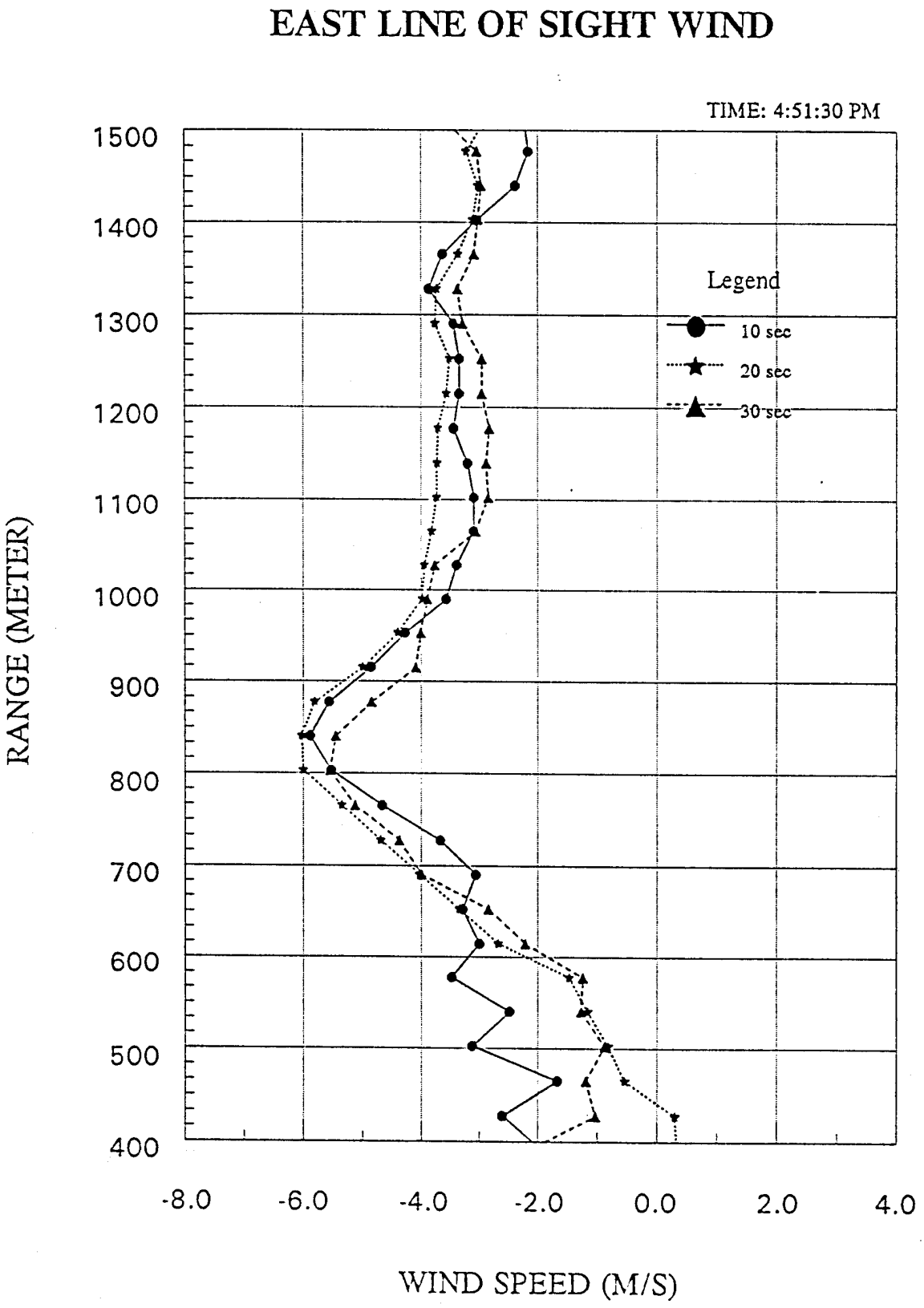

Figure 13 - Line of sight wind profiles obtained with the edge technique lidar. Three consecutive profiles, each taken from a 10-second average, are shown beginning at 4:51:30 p.m.

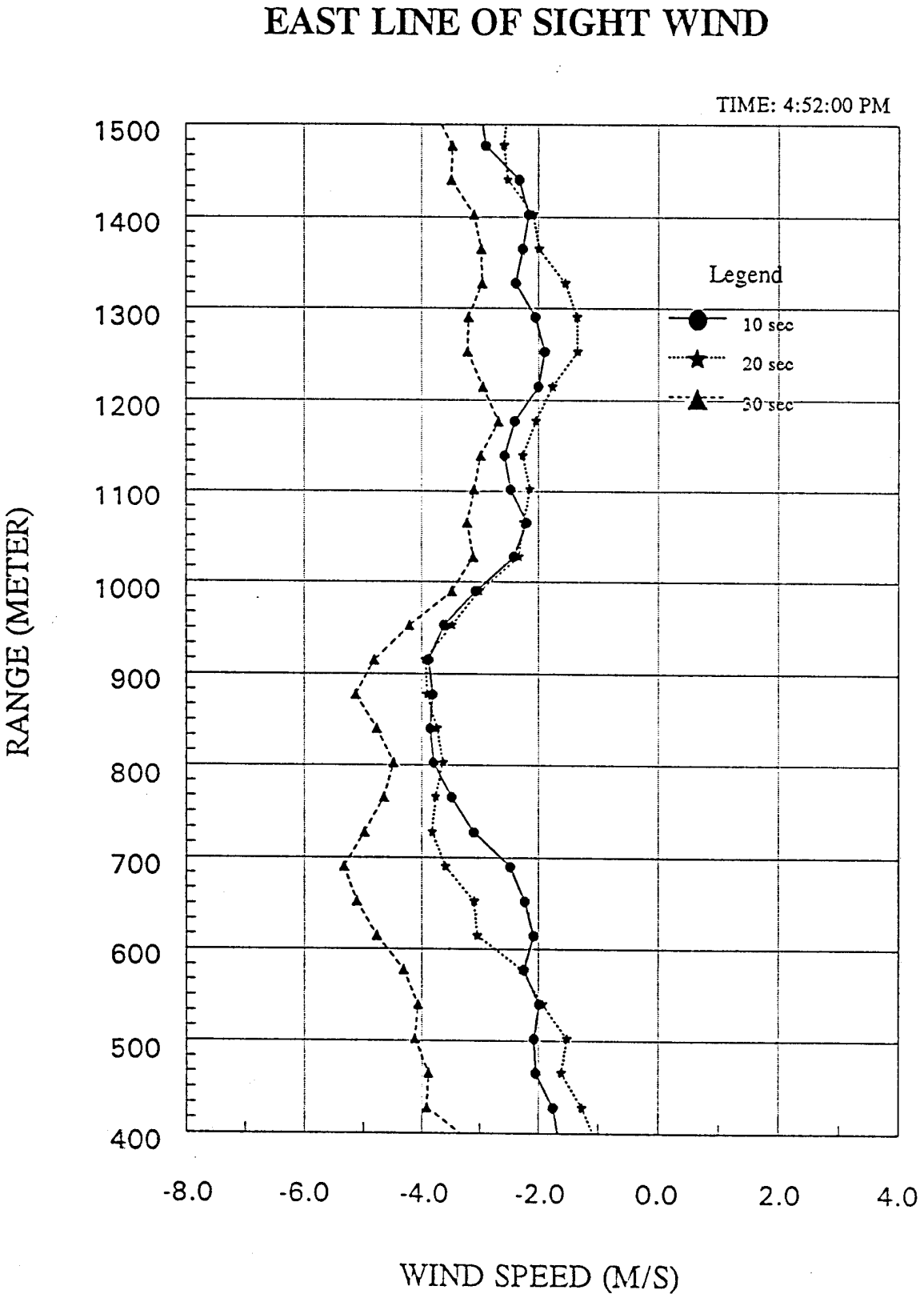

Figure 14 - Line of sight wind profiles obtained with the edge technique lidar. Three consecutive profiles, each taken from a 10-second average, are shown beginning at 4:52:00 p.m.

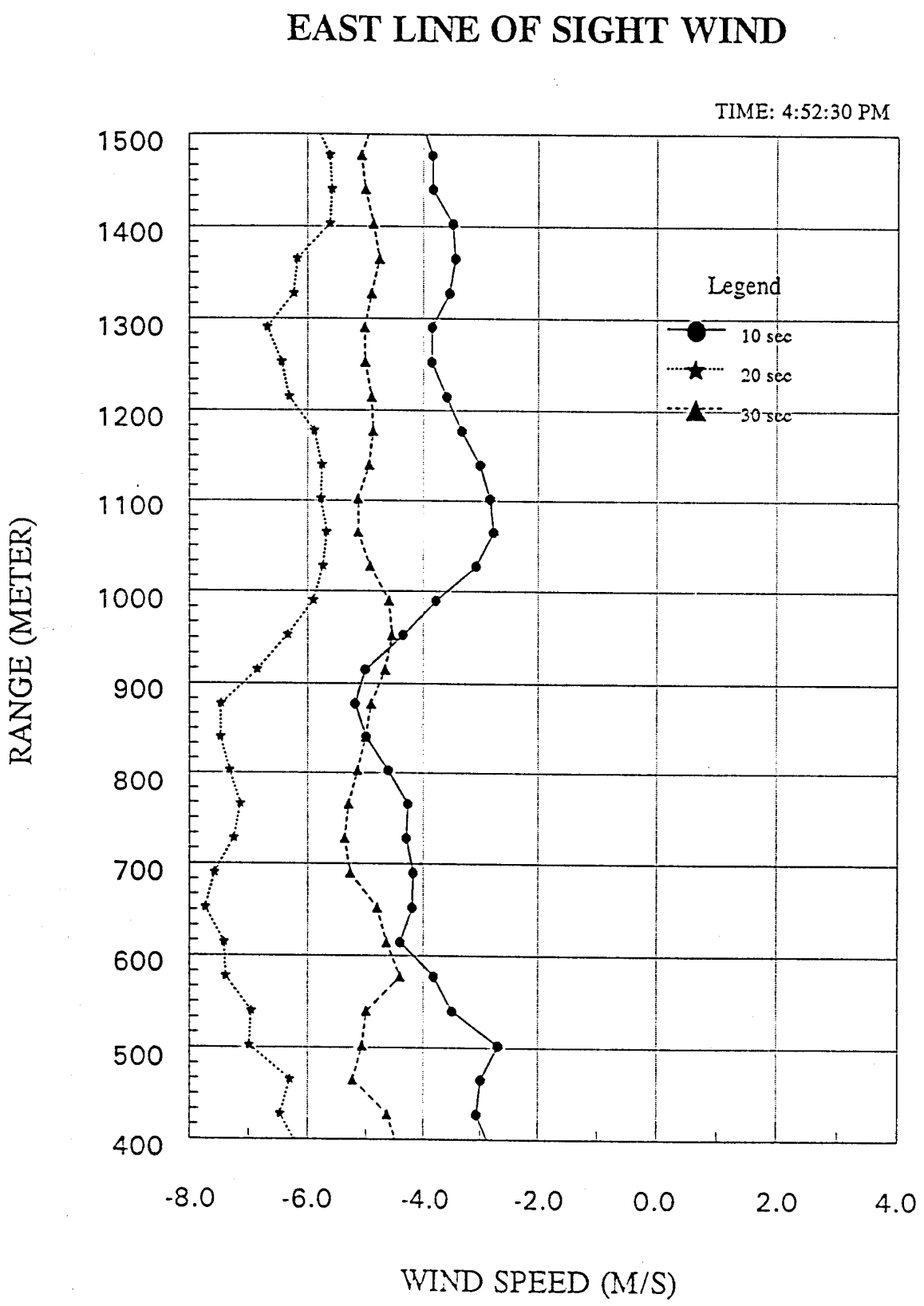

Figure 15 - Line of sight wind profiles obtained with the edge technique lidar. Three consecutive profiles, each taken from a 10-second average, are shown beginning at 4:52:30 p.m.

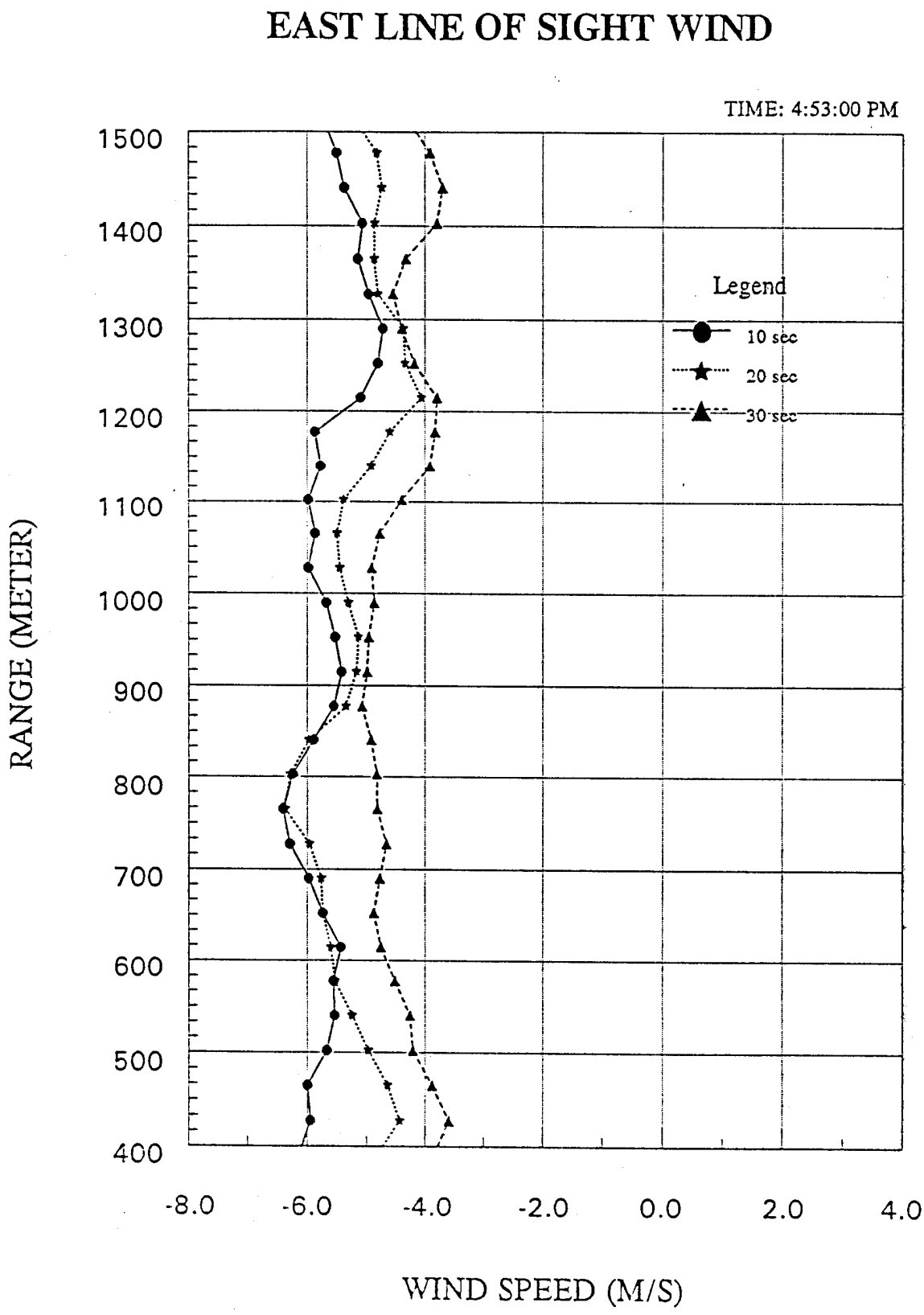

Figure 16 - Line of sight wind profiles obtained with the edge technique lidar. Three consecutive profiles, each taken from a 10-second average, are shown beginning at 4:53:00 p.m.